J Mater Sci (2010) 45:3538–3546
DOI 10.1007/s10853-010-4396-5

Modeling of conductivity in carbon fiber-reinforced cement-based composite

Jing Xu · Wenhui Zhong · Wu Yao

Received: 1 November 2009 / Accepted: 8 March 2010 / Published online: 23 March 2010

Abstract Carbon fiber-reinforced cement is a multifunctional composite material owing to its conductive behavior. This article presents a model for quantitative analysis of the conductive mechanism. The model is based on the concept that the electronic conduction dominates when the composite is in dry state and is a combination of ohmic continuum conduction and tunnel transmission conduction. Therefore, Ohm's law and tunneling effect theory are employed in the modeling process. Validity of the model has been confirmed by comparison of the calculated and measured results. Furthermore, the model is applied in simulating the strain sensing characteristics. Numerical results are shown and compared with measured data obtained under compressive loading. The agreement between theoretical and experimental results provides further support to the model.

Introduction

As a complicated heterogeneous composite material, carbon fiber-reinforced cement is of great technological interest due to the combination of good structural properties and exceptional electrical properties. The addition of short carbon fibers to cement enhances not only the tensile ductility, flexural strength, and toughness but also the electrical conductivity [1–6]. Besides, the composite is more attractive for its multifunctional behavior, which derives from its electrical property, including strain sensing, temperature sensing, piezoresistivity effect, thermoelectric effect, and joule heating [7–12].

The electrical conduction in carbon fiber-reinforced cement involves ions, electrons and/or holes and comprises three types of conduction [13, 14]. In the case of ions, there is only one type of conduction, which is associated with the motion of ions (such as Ca^{2+}, K^{+}, Na^{+}, OH^{-}, etc.) in pore solution. Ionic conductivity varies in a particularly wide range when cement contains a substantial amount of free water. Under dry condition, the cement matrix approximates an insulating material. In the case of electrons and/or holes, there can be two types of conduction—one associated with the motion of electrons and/or holes through the conductive paths formed by a large amount of carbon fibers which are tiny and contact each other, and the other associated with the transmission conduction of electrons between two disconnected fibers that are close enough. The transmission conduction is dominated by the tunneling effect. These types of conduction modes coexist in carbon fiber–cement composite, but they are not independent. The contribution of each type of conduction is not the same for different fiber content. For instance, the moving of electrons and/or holes through continuous fibers, or designated as ohmic continuum conduction mode, dominates when fiber volume fraction is higher than the percolation threshold, thus resulting in a conductive network. In contrast, the electrons' transmission plays an important role when fiber volume fraction is below the percolation threshold or falls within the percolation transition zone.

Although numerous researches concerning the conductive mechanism of carbon fiber-reinforced cement have been reported previously, quantitative work is scant. Quantitative work is very important for fundamental

J. Xu (✉) · W. Zhong · W. Yao
Key Laboratory of Advanced Civil Engineering Materials (Tongji University), Ministry of Education, Shanghai 200092, China
e-mail: 0610060014@tongji.edu.cn

understanding of the conductive mechanism. Hence, the main objective of this article is to investigate the conductive mechanism of carbon fiber–cement mortar in theory, followed by modeling of the conductive behavior. Ohm's law and tunneling effect theory are employed in this theoretical study and analytic results are subsequently compared with experimental data. A related objective is to assess numerically the strain sensitivity of carbon fiber–cement mortar-based on the model.

Modeling

Basic assumptions

In order highlight the issue of conductive mechanism of the carbon fiber–cement mortar, some complicated factors originating from the heterogeneous property of the composite are minimized. Thus, several assumptions are proposed as below:

1. Due to the high resistivity of cement matrix in dry state (10^5–10^7 Ω m), the ionic conduction through pore solution is negligible [15]. Charge carriers, mainly the electrons and/or holes, move only in the most convenient way, either by contacting fibers or by tunnel transmission.

2. The distribution of fibers in cement is completely uniform, namely, there is no clustering nor winding. Fibers are in random of orientation.

3. Charge carriers are regarded as the same for the cases of ohmic continuum conduction and tunnel transmission conduction. The mobility of carriers depends on the intensity of electric field exclusively. Yet, the passing probability of carriers satisfies Schrödinger's equation for tunnel transmission conduction.

Based on the assumptions proposed above, the total resistance of carbon fiber–cement mortar is composed of the ohmic continuum resistance and the tunnel transmission resistance. Assuming that the former is connected in series with the latter, they are denoted as R_C and R_T, respectively. Hence, the primary objective of modeling is the calculation of R_C and R_T.

Ohmic continuum resistance R_C

First, the number of contacting fibers should be determined. Let the fiber volume fraction be V_0, the number of all the fibers in the specimen be N. Then, the relationship between V_0 and N is

$$bhLV_0 = \frac{\pi}{4}d^2 lN \tag{1}$$

where b, h, and L are the width, height, and length of the specimen, respectively; d and l are the diameter and length of a carbon fiber, respectively. The expression of N is denoted as

$$N = \frac{(4bhLV_0)}{(\pi d^2 l)} \tag{2}$$

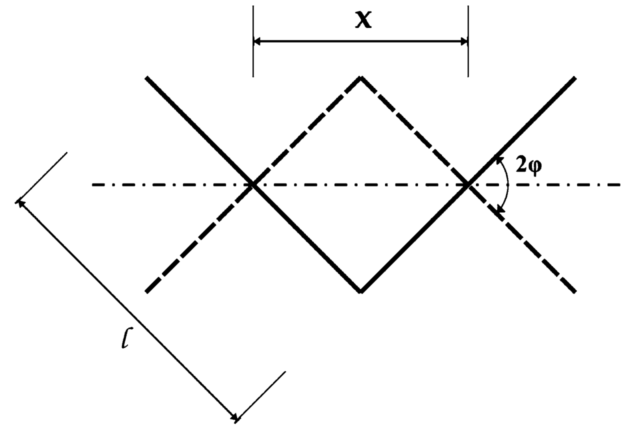

Fig. 1 Schematic illustration of rotational contacting probability of two carbon fibers in a plane

For simplicity, a two-dimensional case is considered. The probability of contact between two single fibers depends on the distance x between the centroids of the fibers, as shown in Fig. 1. If the distance is greater than fiber length, then the two fibers never contact; otherwise, there exists a rotational range in which the two fibers connect. Thus, the probability of contacting can be defined as

$$P = \frac{2\varphi}{\pi} \tag{3}$$

where $\varphi = \cos^{-1}\left(\frac{x}{l}\right)$ is half the rotational angle of the fiber. Equation 3 can be rewritten as

$$P = \frac{2\cos^{-1}\left(\frac{x}{l}\right)}{\pi} \tag{4}$$

Let us assume that the distance x is the average spacing between fibers, and let S be the average spacing. The expression of S can be obtained based on theoretical study of James and James [16]

$$S = 13.8d\sqrt{\frac{1}{V_0}} \tag{5}$$

Then Eq. 4 becomes

$$P = \frac{2\cos^{-1}\left(\frac{13.8d}{l}\sqrt{\frac{1}{V_0}}\right)}{\pi} \tag{6}$$

Let the number of contacting fibers be N_C which can be expressed by the equation

$$N_C = N \cdot P \tag{7}$$

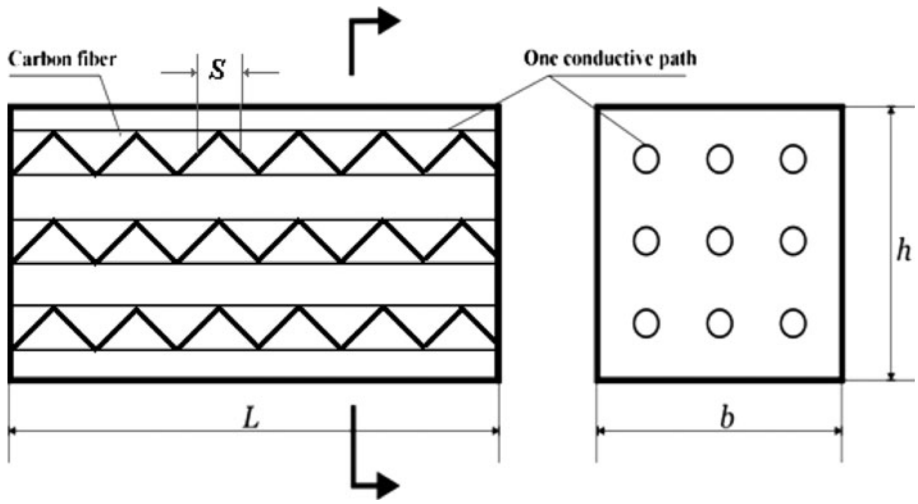

Fig. 2 Schematic illustration of conductive paths formed by contacting carbon fibers in the longitudinal and cross-sectional direction

Substituting Eqs. 2 and 6 into Eq. 7 yields

$$N_C = \frac{8bhL\,V_0 \cos^{-1}\left(\frac{13.8d}{l}\sqrt{\frac{1}{V_0}}\right)}{(\pi d)^2 l} \quad (8)$$

Suppose the contacting fibers form a magnitude of continuous conductive paths in the longitudinal direction of the specimen, which is parallel to the orientation of electric field. Conductive paths are uniformly distributed at any section, and the contacting fibers are connected in an ideal state as shown in Fig. 2. For this pattern, the spacing of any of two neighboring fibers is S, and fibers are connected end-to-end. Let the number of fibers per conductive path is N_A and the number of conductive paths is N_P. The expression of N_A is

$$N_A = \frac{L}{S} \quad (9)$$

Accordingly, the resistance R_c of one conductive path is

$$R_C = \frac{\rho l}{\frac{\pi}{4}d^2} \cdot \frac{L}{S} \quad (10)$$

where ρ is the resistivity of carbon fiber. The ohmic continuum resistance R_C can be regarded as a series of identical resistance R_c connected in parallel, with a total number of N_P. It is obvious that N_P can be expressed as follows:

$$N_P = \frac{N_C}{N_A} \quad (11)$$

Hence, the expression of R_C is

$$R_C = \frac{1}{N_P} R_C \quad (12)$$

Substituting Eqs. 5 and 8–11 into Eq. 12, we obtain

$$R_C = \frac{\pi \rho l^2 L}{380.88bhd^2 \cos^{-1}\left(\frac{13.8d}{l}\sqrt{\frac{1}{V_0}}\right)} \quad (13)$$

We should also allow for the influence of contact resistance in the model. Assuming that the total contact resistance, the contact resistance in one conductive path, the contact resistance between two neighboring fibers are R_J, R_j, R_{j0}, respectively. Similarly, we have the relationship among R_J, R_j, and R_{j0} as follows:

$$R_J = \frac{1}{N_P} R_j = \frac{1}{N_P} \cdot \frac{L}{S} \cdot R_{j0} \quad (14)$$

Incorporating Eq. 14 into Eq. 13

$$R_C = \frac{\pi l L}{380.88bh \cos^{-1}\left(\frac{13.8d}{l}\sqrt{\frac{1}{V_0}}\right)}\left(\frac{\rho l}{d^2} + \frac{\pi}{4}R_{j0}\right) \quad (15)$$

The contact resistance R_{j0} depends on the contact with each other state of two neighboring fibers. Suppose that the two fibers are in perfect contacting, which can be described as one single point contact and the contacting region is a circle. In addition, no insulating film is found on the fiber surface. Then, the contact resistance R_{j0} can be approximately estimated as [17]

$$R_{j0} = \frac{\rho}{2}\sqrt{\frac{\pi \delta H}{kF}} \quad (16)$$

where H is the hardness of carbon fiber, F the axial force applied on the contacting region, δ the deformation coefficient of carbon fiber, and k the number of contacting points. Substituting Eq. 16 into Eq. 15 we have

$$R_C = \frac{\pi \rho l L}{380.88bh \cos^{-1}\left(\frac{13.8d}{l}\right)}\left(\frac{l}{d^2} + \frac{\pi}{8}\sqrt{\frac{\pi \delta H}{nF}}\right) \quad (17)$$

Tunnel transmission resistance R_T

The conduction of carbon fiber cement composite involves numerous charge carriers transmitting between two fibers. According to basic assumption (2), the value of spacing between any two fibers not contacting follows a normal distribution. For ease of calculation, the probability density

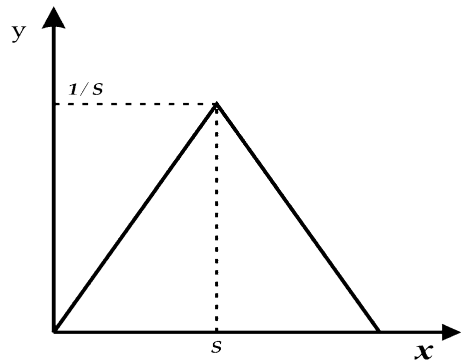

Fig. 3 Simplified probability density function of fiber spacing distribution

function of fiber spacing distribution is defined as piecewise linear function, as shown in Fig. 3. The distribution of fiber spacing follows the function as below:

$$\begin{cases} y = \frac{1}{S^2}x & 0 \le x \le S \\ y = \frac{2}{S} - \frac{1}{S^2}x & S < x \le 2S \end{cases} \tag{18}$$

It is well known that width of the barrier has a great influence on the transmission current. Here, the fiber spacing represents the width of the barrier. The tunneling current approaches 0 if fiber spacing exceeds a critical value. Because carriers still find the most convenient way even if tunnel transmission conduction is involved, the equivalent tunnel transmission resistance R_T can be divided into a large number of tiny resistors connected in parallel. Figure 4 shows the proposed circuit model, in which R_{Ti} represents a resistor that is equivalent to the tunnel transmission resistance with a specific fiber spacing in

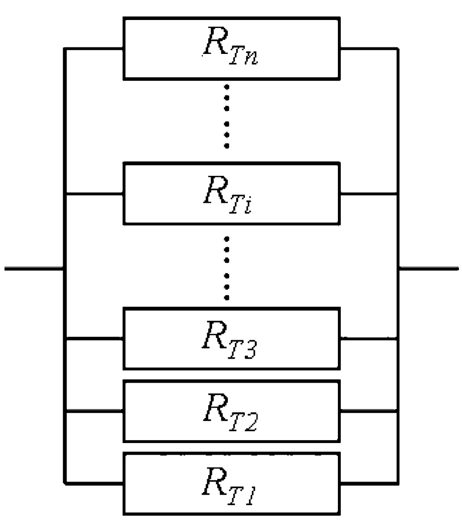

Fig. 4 Equivalent electric circuit model used for the calculation of tunnel transmission resistance

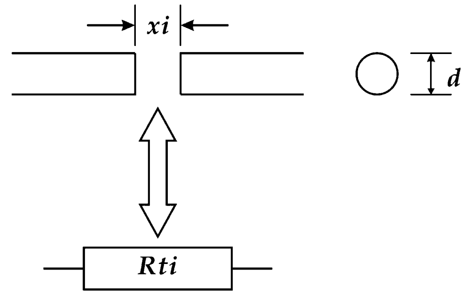

Fig. 5 Schematic illustration of one pure resistor being representative of tunneling

the range of tunnel transmission conduction. Therefore, R_T can be expressed by the following equation:

$$\frac{1}{R_T} = \frac{1}{R_{T1}} + \cdots + \frac{1}{R_{Ti}} + \cdots + \frac{1}{R_{Tn}} \tag{19}$$

where R_{Ti} is regarded as a pure resistor with x_i being the length and $\frac{\pi}{4}d^2$ being the cross-sectional area, as shown in Fig. 5. The expression of R_{Ti} should be

$$R_{Ti} = \frac{\rho_{Ti}\,x_i}{\frac{\pi}{4}d^2} \tag{20}$$

where ρ_{Ti} is the corresponding resistivity. On the basis of Ohm's law, we have

$$\rho = \frac{1}{\sigma} = \frac{1}{nq\mu} \tag{21}$$

where σ is the conductivity of carbon fiber, n the total number of charge carriers, q the electric charge amount of the carrier, and μ is the mobility of the carrier. Similarly, ρ_{Ti} can be expressed as

$$\rho_{Ti} = \frac{1}{\sigma_{Ti}} = \frac{1}{n_{Ti}q_{Ti}\mu_{Ti}} \tag{22}$$

According to basic assumption (3), the property of carriers moving through contacting fibers and transmitting between two adjacent fibers is the same in essence. In other words, the electric charge amount q and the mobility μ are equal under both of the conditions. However, there exists a passing ratio for carriers in tunnel transmission conduction because carriers need to hop through a barrier with width of x_i. Thus, Eq. 22 can be rewritten as

$$\rho_{Ti} = \frac{1}{n_{Ti}\,q\mu} \tag{23}$$

Dividing Eq. 21 by Eq. 23 yields

$$\rho_{Ti} = \frac{n}{n_{Ti}}\rho = \frac{1}{T_i} \tag{24}$$

in which T_i is the transmission coefficient of the charge carrier with energy of E hopping through a barrier of width x_i and height U_0. The expression of T_i is given by

$$T_i = \frac{4E}{U_0} e^{\frac{2}{\hbar}\sqrt{2m(U_0 - E)}x_i} \quad (25)$$

where m is the mass of the charge carrier, and $\hbar$ is the reduced Plank's constant. Substituting Eqs. 24 and 25 into Eq. 20 yields

$$R_{Ti} = \frac{\rho U_0 x_i}{\pi d^2 E} e^{\frac{2}{\hbar}\sqrt{2m(U_0 - E)}x_i} \quad (26)$$

The calculation of R_T is made with the aid of integral method and then taking into account the probability density function discussed previously. If probability of R_{Ti} within the region of (x_i, x_{i+1}) is $\frac{1}{S^2}x_i\,dx$, then the number of R_{Ti} should be $\frac{1}{S^2}N' x_i dx$, where N' represents the counts of pairs of non-contacting fibers. Thus, the expression of R_T is given by

$$R_T = \left(\int_0^a \frac{N'\pi d^2 E}{S^2 \rho U_0} e^{-\frac{2}{\hbar}\sqrt{2m(U_0-E)x}} dx\right)^{-1} \quad (27)$$

where a is the upper limit of barrier width for effective tunnel transmission conduction.

We shall next determine the parameter N' in Eq. 27. The counts of pairs of non-contacting fibers relates to the number of non-contacting fibers and the number of fibers around one single fiber; let the former be N_t and the latter be N_a. Obviously, N_t can be expressed as

$$N_t = N(1 - P) \quad (28)$$

N_a can be obtained using the theory of crowding factor proposed by Kerekes and Schell [18]. The crowding factor has been employed to characterize the fiber flocculation, and it is the number of fibers in a sphere the diameter of which equals to the length of one single fiber. N_a is expressed as

$$N_a = \frac{2}{3} V_0 (1 - P) \left(\frac{l}{d}\right)^2 \quad (29)$$

Since the relationship among N', N_t and N_a be

$$N' = \frac{N_t \cdot N_a}{2} \quad (30)$$

Then, we can obtain N' by substituting Eqs. 2, 6, 28 and 29 into Eq. 30

$$N' = \frac{4bhlLV_0^2}{3\pi d^4} \left(1 - \frac{2\cos^{-1}\left(\frac{13.8d}{l}\sqrt{\frac{1}{V_0}}\right)}{\pi}\right)^2 \quad (31)$$

Substituting Eqs. 5 and 31 into Eq. 27, we obtain the expression of R_T

$$R_T = \frac{142.83\rho U_0 d^4 \beta e^{\alpha\beta}}{bhlLEV_0^3(e^{\alpha\beta} - 1)} \left(1 - \frac{2\cos^{-1}\left(\frac{13.8d}{l}\sqrt{\frac{1}{V_0}}\right)}{\pi}\right)^{-2} \quad (32)$$

where $\beta = \frac{2}{\hbar}\sqrt{2m(U_0 - E)}$.

Experimental details

Materials and specimens

Carbon fibers were isotropic PAN-based, unsized, with length of 5 mm, as obtained from Shanghai Carbon Corporation. The fiber properties are shown in Table 1. Ordinary Portland cement which corresponds to ASTM Type I was used throughout. The sand used was local natural sand with specific gravity of 2.65. Silica fume was used along with fibers to improve the dispersion of fibers in cement mortar. The silica fume (Elkem Materials) was used in the amount of 15% by mass of cement. The defoamer, used in the amount of 0.13 vol.%, was tri-butyl phosphate. The water-reducing agent (Kao Chemical Corporation, 21 s; polycarboxylic type water-reducer) was used in the amount of 1.0% by mass of cement. Water/cement (w/c) ratio was 0.45 (by mass) and sand/cement (s/c) ratio was 1.0 (by mass).

Specimens containing 0.05, 0.10, 0.15, 0.20, 0.25, and 0.40% by volume of fibers were prepared under laboratory conditions. A rotary mixer with a flat beater was used for mixing. Fibers were added in water, and then the defoamer, and water-reducing agent were added and mixed for about 1 min. Then the mixture, cement, sand, and silica fume were mixed in the mixer for 3 min. After pouring the mixture into molds, an external vibrator was used to facilitate compaction and decrease the amount of air bubbles. The specimens were demolded after 24 h and then cured in a moist-curing room for 28 days. In order to make sure the completely dry state, all the specimens were heated to 105 °C for 6 h and then put in a desiccator at room temperature.

Testing

Electrical resistivity measurements were conducted using the four-probe method, with silver paint in conjunction

Table 1 Properties of carbon fiber

Diameter (μm)	Density (g cm^{-3})	Tensile strength (GPa)	Young's modulus (GPa)	Elongation at break (%)	Carbon content (wc%)	Electrical resistivity (μΩ m)
7 ± 0.2	1.78	>3.0	220–240	1.25–1.60	>95	15

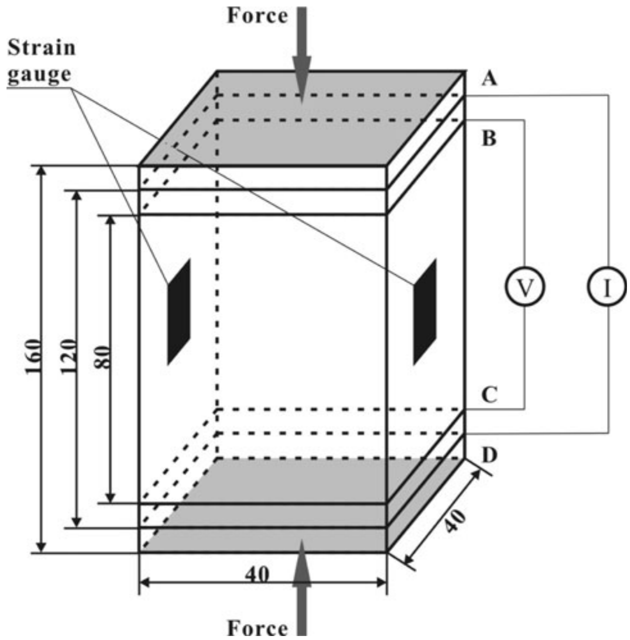

Fig. 6 Specimen configuration for measurements

with copper wires for electrical contacts. Two Fluke 189 multimeters were used. Specimens were in the form of rectangular bars of size 40 mm × 40 mm × 160 mm, each consisting four electrical contacts placed perimetrically around the specimen in four parallel planes perpendicular to the length of the specimen. The four contacts, labeled A, B, C, and D, were such that A and D (120 mm apart) were for passing current, and B and C (80 mm apart) were for voltage measurement. Figure 6 depicts the configuration of the specimen for electrical measurements.

Compressive stress was applied on the entire 40 mm × 40 mm cross section of the specimen for the purpose of measuring the longitudinal resistance under compression in the same direction. Loading was provided by a hydraulic mechanical testing system (Instron 8501), and the loading rate was fixed at 3 kN s^{-1}. Two strain gages were attached to the center of the specimen, one on each of two opposite surfaces, as illustrated in Fig. 6. During compressive testing, DC electrical resistance measurement was made in the stress axis, using the four-probe method.

Results and discussion

Comparison of measured and calculated resistance values

From the experimental work with the specimen size shown in Fig. 6, involves $b = 40$ mm, $h = 40$ mm, and $L = 80$ mm. The hardness H of carbon fiber is 500 MPa [19]. The axial force F at the contacting point is assumed as the gravity of one single fiber which is 3.43×10^{-9} N. Value of 0.2 is assigned to the deformation coefficient δ of contacting region in the elastic deformation state. k is 1 for the one single point contact. The reduced Plank's constant $\hbar$ is $1.053 \times 10^{-34} \mathrm{m}^2$ kg s^{-1}. The mass of charge carrier $m = 9.11 \times 10^{-31}$ kg because carriers are mainly electrons in carbon fibers. Energy of carrier E depends on the activation energy of electrons in fibers. Meanwhile, the effect of the applied voltage on the carrier energy should be evaluated. Suppose the applied voltage is V, then the electric field intensity ξ is

$$\xi = \frac{V}{L} \tag{33}$$

In this electric field, charge carriers would attain velocity v, and its direction is related to the electric field. The velocity vector $\boldsymbol{v}$ can be given by the following expression:

$$v = \mu\xi \tag{34}$$

If cement paste is regarded as an approximate semiconductor, then the value of carrier mobility should be in the range of 10–100 m^2 (V s)$^{-1}$ [20]. From an energy point of view, the charge carrier gains an extra kinetic energy E_v, which can be written as

$$E_\mathrm{v} = \frac{1}{2}mv^2 \tag{35}$$

Thereby, the energy E of the charge carrier in the electric field of intensity ξ should be

$$E = E_0 + E_v \tag{36}$$

where E_0 is the energy of the charge carrier free from electric field, which is essentially the activation energy of the fiber. Based on prior study on the activation energy related to carbon fiber grade, a value of 0.36 eV was used in this case due to PAN-based carbon fiber being amorphous type [21]. Substituting Eqs. 33–35 into Eq. 36 results in the following expression:

$$E = E_0 + \frac{m\mu^2 V^2}{2L^2} \tag{37}$$

Charge carrier energy values with different applied voltages for three levels of carrier mobility are given in Table 2. If the applied voltage is below 5 V, then it has negligible impact on the carrier energy. During the tests, the voltage applied was within 3 V, thus we can treat the value of carrier energy as a constant, i.e., 0.36 eV.

Values in the range between 0.36 and 0.72 eV (i.e., U_0/E between 1 and 2) were assigned to the height of barrier U_0. The width of barrier a was set equal to 0.5 nm when the value of U_0/E is in the range of 1–2 [22]. Substituting these parameters into Eqs. 17 and 32, we obtain result of total resistance.

Table 2 Charge carrier energy with different applied voltages for three levels of carrier mobility

Applied voltage (V)	Carrier energy (eV)		
	Carrier mobility (m^2 (V s)$^{-1}$)		
	10	50	100
0.1	0.3600	0.3600	0.3600
0.5	0.3600	0.3600	0.3600
1	0.3600	0.3600	0.3600
5	0.3600	0.3600	0.3601
10	0.3600	0.3601	0.3604
50	0.3601	0.3628	0.3711
100	0.3604	0.3711	0.4045

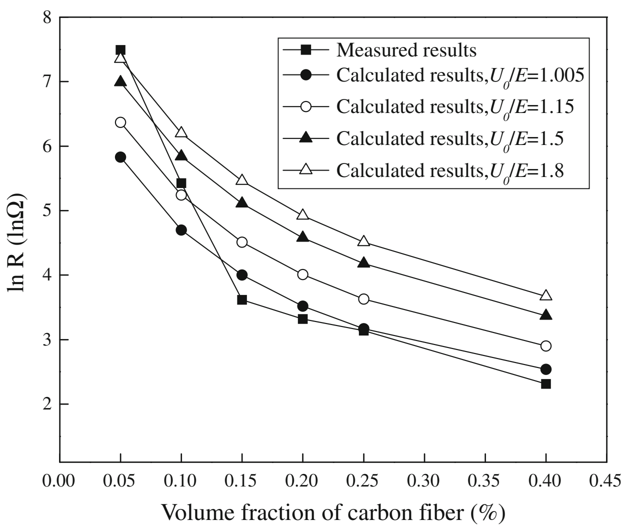

Fig. 7 Comparison of measured and calculated values of resistance at different U_0/E

Comparison of measured and calculated values at different U_0/E is shown in Fig. 7. The calculated results show that minor changes of U_0/E have a marked influence on the total resistance values, although the shapes of curves are similar. When U_0/E is 1.005, good agreement is observed between the calculated and measured results for the cases of high volume fractions, but not for the cases of lower ones, especially far below the percolation threshold (i.e., volume fraction of 0.05%) [23]. However, at higher U_0/E values, calculated results are nearly in agreement wit measured results for low fiber fractions. This phenomenon is attributed to the dependence of tunneling barrier height on the carbon fiber content. There is a possible correlation between barrier height and barrier width, i.e., the fiber–fiber distance.

Table 3 shows the measured and calculated values of resistance at different fiber fractions. Both R_C and R_T are found to decrease monotonically with increasing fiber content. The contribution of R_C to the total resistance R is rather lower than that of R_T when fiber content is below the percolation threshold. While the fiber content increases to the vicinity of percolation threshold (volume fraction of 0.40%), the fraction of R_C is highly significant. It should also be pointed out that the contact resistance R_J has a great effect on R_C and, therefore, cannot be neglected.

Modeling of strain-sensing ability

The ability of carbon fiber-reinforced cement composite to sense its own strain and damage is important for smart structures and buildings. Simply using DC electrical resistance measurement, embedded or attached sensors can be applied for structural vibration control, traffic monitoring, weighing, and building security [24, 25]. The advantages of this self-sensing propertyincludes low cost, high durability, and compatibility with structural materials. Chung et al. [26, 27] investigated self-sensing of cement based materials and attributed this piezoresistive effect to slight fiber pull-out of crack-bridging fibers during tension and fiber push-in upon compression. In this study, we tried to explain this phenomenon based on the tunneling theory.

Consider a carbon fiber-reinforced cement specimen under uniaxial tension or compression in the elastic regime, such that the strain resulting from the applied loading in the longitudinal distance is ε. The sign of ε is positive for tension and negative for compression. We assume that part of the strain causes the change in fiber spacing. Let Φ be

Table 3 Comparison of measured and calculated resistance values

Volume fraction of fiber (%)	R_J (Ω)	R_C (Ω)	R_T (Ω)	R (Ω)	R' (Ω)	R_C/R (%)	R_C/R' (%)
0.05[a]	7.00	12.98	1541.46	1554.44	1791.84	0.84	0.73
0.10[b]	4.04	7.50	180.62	188.12	227.59	3.40	3.30
0.15[c]	3.52	6.53	48.18	54.71	37.27	11.94	17.53
0.20[c]	3.29	6.09	27.78	33.87	27.64	17.99	22.05
0.25[c]	3.15	5.83	18.03	23.87	23.09	24.45	25.27
0.40[c]	2.93	5.44	7.19	12.63	10.10	43.05	53.82

[a] U_0/E is 1.8, [b] U_0/E is 1.15, [c] U_0/E is 1.005

the percentage of strain. Assuming that each of the fiber spacing contributes equally to the strain and letting Δa be the distance change, we have

$$\Phi \varepsilon L = \Delta a N' \quad (38)$$

Thus, we obtain

$$\Delta a = \frac{\Phi \varepsilon L}{N'} \quad (39)$$

From Eq. 39, we know that Δa shares the same as sign as ε. Then, the tunnel transmission resistance R_{T} is

$$R_{\mathrm{T}} = \left(\int_0^a \frac{N' \pi d^2 E}{S^2 \rho U_0} e^{-\frac{2}{\hbar}\sqrt{2m(U_0 - E)}(x + \Delta a)}\, dx \right) \quad (40)$$

Substituting Eq. 39 into Eq. 40, we obtain

$$R_T = \frac{190.44 \rho U_0 \beta e^{a\beta}}{\pi E V_0 N' (e^{a\beta} - 1)} e^{\frac{\Phi \beta L}{N'} \varepsilon} \quad (41)$$

The total resistance would be

$$R = R_{\mathrm{C}} + R_{\mathrm{T}} \quad (42)$$

Under the condition of fixed fiber content, we can use the following equation as short form of R

$$R = A + B e^{C\varepsilon} \quad (43)$$

It is found in Eq. 43 that the total resistance is an exponential function of strain. A and B represent ohmic continuum resistance and tunnel transmission resistance without loading, respectively.

Owing to minor damage that occurred to cement matrix during compressive loading, the measured resistance is usually irreversible after the first cycle, but it stabilizes after several cycles of loading and unloading. Based on this effect, measurement of resistance was not conducted until the fourth cycle of compressive loading was applied. Assuming the value of Φ as 100%, we observe that the strain contributes to the fiber spacing change completely. Figure 8 shows the comparison of the measured and the calculated fractional resistance values versus strain, and the stress values versus strain. The calculated results agree well with the measured data, although some difference is observed at relatively high strain values. The high strain causes microcracking in cement, which in turn results in the redistribution of fibers. This can influence the tunnel transmission conduction to some extent. Table 4 shows the measured and calculated fractional resistance values at −650 microstrain. It can be observed that the fractional resistance, whether measured or calculated, decreases along with increasing fiber content. This is in accordance

Table 4 Measured and calculated fractional resistance values at −650 microstrain

Fiber volume fraction (%)	Measured $\Delta R/R$	Calculated $\Delta R/R$
0.05	−23.9	−19.6
0.15	−16.2	−15.9
0.25	−5.7	−5.5
0.40	−0.62	−0.48

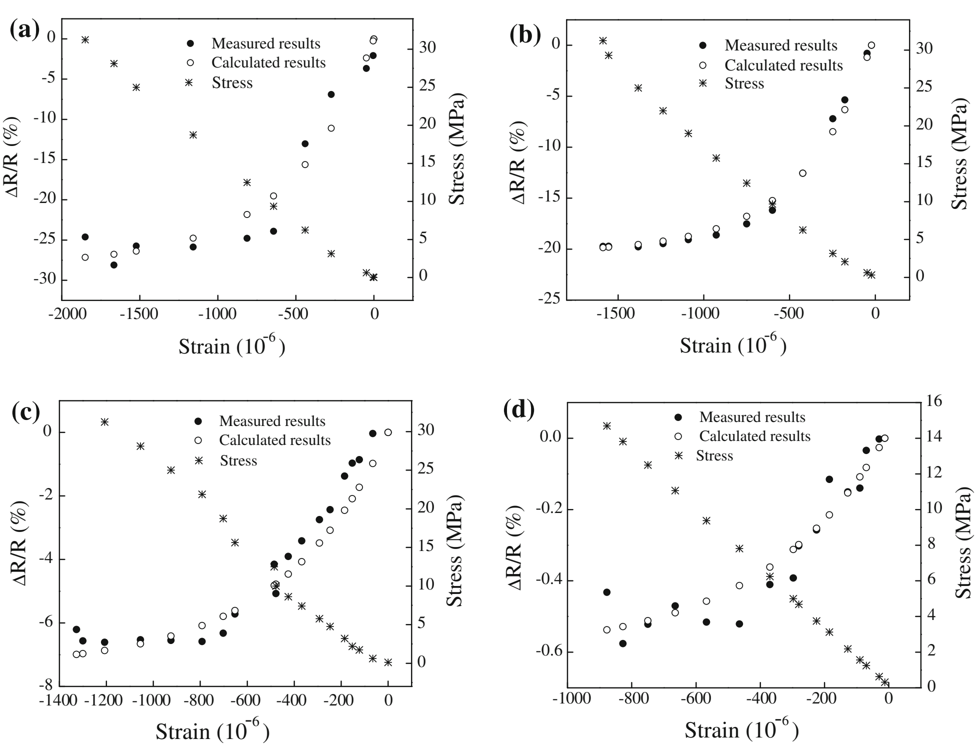

Fig. 8 Comparison of measured and calculated values of fractional resistance versus strain and stress values versus strain at different fiber volume fractions. **a** 0.05%, **b** 0.15%, **c** 0.25%, **d** 0.40%

with the gauge factor proposed in Ref. [11]. The gauge factor in longitudinal direction decreases as the fiber content increases in the region of both below and in the vicinity of percolation threshold.

Conclusions

A model for quantitatively analyzing the conductive mechanism of carbon fiber reinforced cement mortar is provided, based on the notion that the electrical behavior is mainly contributed by electronic conduction. The conduction is due to the contact of fibers and the tunnel transmission. Good agreement between model and experiment was attained by selecting appropriate values of parameters. Subsequently, the model was applied to simulating the strain-sensing ability in the process of compressive loading. The agreement between the measured and calculated results provides further support to the model presented here.

Acknowledgements The authors would like to acknowledge the financial support for this study from the National Natural Science Foundation of China (No. 50238040) and the Program for Young Excellent Talents in Tongji University.

References

1. Park SB, Lee BI, Lim YS (1991) Cem Concr Res 21(4):589
2. Banthia N, Djeridane S, Pigeon M (1992) Cem Concr Res 22(5):804
3. Chung DDL (2000) Smart Mater Struct 9(4):389
4. Reza F, Batson GB, Yamamuro JA, Lee JS (2001) ACI Mater J 98(1):25
5. Chen B, Liu JY, Wu KR (2005) Cem Concr Res 35(11):2183
6. Chiarello M, Zinno R (2005) Cem Concr Compos 27(4):463
7. Chung DDL (2001) J Mater Sci 36(6):1315. doi:10.1023/A:1017522616006
8. Chung DDL (2000) Compos B Eng 31(6–7):511
9. Sun M, Li Z, Mao Q, Shen D (1998) Cem Concr Res 28(4):549
10. Wang S, Wen S, Chung DDL (2004) Adv Cem Res 16(4):161
11. Wen S, Chung DDL (2005) ACI Mater J 102(4):244
12. Sun MQ, Liu QP, Li ZQ, Hu YZ (2000) Cem Concr Res 30(10):1593
13. Wen SH, Chung DDL (2006) Carbon 44(11):2130
14. Cao JY, Chung DDL (2004) Cem Concr Res 34(3):481
15. Hansson ILH, Hansson CM (1983) Cem Concr Res 13(5):675
16. Romualdi JP, Mandel JA (1964) J Am Concr Inst 61:657
17. Holm R (1979) Electric contacts: theory and application, 4th edn. Springer, Berlin
18. Kerekes RJ, Schell CJ (1992) J Pulp Paper Sci 18(1):32
19. Ramanathan T, Schulz E, Subramanian K (2005) Compos Sci Technol 65(1):1
20. Wlof HF (1971) Semiconductors. Wiley, New York
21. Wen SH, Chung DDL (2001) Carbon 39(3):369
22. Schiff LI (1968) Quantum mechanics, 3rd edn. McGraw-Hill, New York
23. Chen B, Wu KR, Yao W (2004) Cem Concr Compos 26(4):291
24. Shi ZQ, Chung DDL (1999) Cem Concr Res 29(3):435
25. Wu B, Huang XJ, Lu JZ (2005) Cem Concr Res 35(7):1430
26. Wen SH, Chung DDL (2006) Cem Concr Res 36(10):1879
27. Zhu SR, Chung DDL (2007) J Mater Sci 42(15):6222. doi:10.1007/s10853-006-1131-3